Correlation of ISO V-Block and Three-Edge Bearing Test Methods

A.P. MOSER

The objective of this study was to correlate crush strengths of various sizes and classes of rigid pipe as determined by two test methods: the three-edge bearing (wood-block) method and the International Standards Organization (ISO) V-block method. In addition, the crush strengths of the various pipe rings were determined by mathematical modeling and analytical solutions via computer programming. The experimentally determined crush strengths were in close agreement with those predicted by the analytical solutions. Crush strengths determined by the ISO V-block method are greater than those determined by the three-edge bearing method on similar pipe rings. That is, the ISO V-block method is less conservative, since it predicts that a pipe will withstand a greater crush load.

Traditionally, the crush load for rigid pipe has been determined by using the three-edge bearing wood-block method of testing. Other test methods have been used. It has long been recognized that the particular test method can have a substantial effect on the resulting crush strengths. The International Standards Organization (ISO) has proposed a so-called V-block method for testing.

The objective of this study was to determine the loads required to cause crush failure for pipe of various sizes and strengths. Asbestos cement pipes were used in the study because of the availability of a wide range of strengths. These crush loads were determined by using the two test methods referred to above. The data on strength variation due to test method were used to predict V-block strength from actual wood-block test data, and vice versa. The use of the data also permits one to calculate how changing from the wood-block test method to the V-block test method influences load factors that have previously been defined by using wood-block test data. Such an exercise is necessary since the load factor (LF) is defined as follows (1, p. 700; 2):

LF = crush failure load as determined by testing in soil in actual burial condition divided by crush load as determined by standard test method.

Obviously, if one changes the standard test method, a change in load factor will result.

ANALYTICAL SOLUTION TO EXTERNALLY LOADED PIPE RING

The problem of an externally loaded circular pipe ring can be considered a plane problem if variations along the pipe axis can be assumed negligible. For such a problem, the governing equation is (3) as follows:

$$\nabla^4\phi(r,\theta) = 0$$

The function $\phi(r,\theta)$ is a plane stress function that satisfies equilibrium if stresses are determined as follows:

$$\sigma_r = [(1/r)(\partial\phi/\partial r)] + [(1/r^2)(\partial^2\phi/\partial\phi^2)]$$

$$\tau_{r\theta} = -(\partial/\partial_r)[(1/r)(\partial\phi/\partial\theta)]$$

$$\sigma_\theta = \partial^2\phi/\partial r^2$$

The requirements for a solution are as follows:

1. $\phi(r,\theta)$ must satisfy $\nabla^4\phi = 0$, and
2. $\phi(r,\theta)$ must satisfy boundary conditions.

The following stress function satisfies $\nabla^4\phi = 0$:

$$\phi = A_0 \ell n r + C_0 r^2 + \sum_{n=2}^{\infty} (A_n r^n + b_n r^{n+2} + C_n r^{-n} + d_n r^{-n+2}) \cos n\theta \quad (1)$$

The constants A_0, C_0, A_n, b_n, C_n, and d_n can be determined in such a manner that the boundary conditions are satisfied. Thus, Equation 1 represents a solution that is exact with respect to initial assumptions. These assumptions are (a) circular ring, (b) no variations along pipe axis, and (c) symmetric loading.

Since the pipe ring geometry is symmetric and a symmetric stress function has been chosen (i.e., symmetric in θ), only half the pipe ring need be considered (Figure 1).

The inner boundary at r = a is traction free. Thus,

$$\left.\begin{aligned}\sigma_r &= 0\\ \tau_{r\theta} &= 0\end{aligned}\right\} \quad \text{at } r = a$$

The outer boundary at r = b is loaded as follows:

$$\text{Top of ring: } -(P/2) = \int_0^{\alpha/2} b\sigma_{r1}\cos\theta\, d\theta \quad (2)$$

$$\text{Bottom reaction: } -(P/2) = \int_{\gamma-\beta/2}^{\gamma+\beta/2} b\sigma_{r2}\cos\theta\, d\theta \quad (3)$$

Here σ_{r1} and σ_{r2} are radial stresses at the top and bottom, respectively. The integration of Equations 2 and 3 results in the following boundary stresses:

$$\sigma_{r1} = -P/(2b\sin\alpha/2) \quad (4)$$

$$\sigma_{r2} = P/2b[\sin(\gamma - \beta/2) - \sin(\gamma + \beta/2)] \quad (5)$$

These boundary stresses can be expressed in a Fourier series. A half-range expansion for a cosine series is as follows:

$$A_n = (2/\pi)\int_0^{\pi} (\sigma r)_{r=b}\cos\theta\, d\theta$$

$$= (2/\pi)\left[\int_0^{\alpha}\sigma_{r1}\cos\theta\, d\theta + \int_{\pi-(\gamma+\beta/2)}^{\pi-(\gamma-\beta/2)}\sigma_{r2}\cos\theta\, d\theta\right] \quad (6)$$

Integrating and substituting the expressions for σ_{r1} and σ_{r2} from the boundary conditions, one obtains

$$a_n = (P/n\pi b)\left(\{[\sin n(\pi - \gamma + \beta/2) - \sin n(\pi - \gamma - \beta/2)] \div [\sin(\gamma - \beta/2) - \sin(\gamma + \beta/2)]\} + [(\sin n\alpha/2)/(\sin\alpha/2)]\right) = Q_n \quad (7)$$

and

$$a_0 = (P/b\pi)\{\beta/[\sin(\gamma - \beta/2) - \sin(\gamma + \beta/2)] - \alpha/(2\sin\alpha/2)\} \quad (8)$$

The following two equations are used to solve for A_0 and C_0:

$$(A_0/b^2) + 2C_0 = a_0/2$$

$$(A_0/a^2) + 2C_0 = 0$$

Thus,

$$A_0 = a_0(ab)^2/2(a^2 - b^2) \qquad C_0 = -a_0 b^2/4(a^2 - b^2) \tag{9}$$

where a_0 is given in Equation 8 above. Four equations in four unknowns (a_n, b_n, c_n, d_n) may be written as follows:

$$a_n b^{n-2}(n - n^2) + b_n b^n(n - n^2 + 2) - c_n b^{-(n+2)}(n + n^2) - d_n b^{-n}(n + n^2 - 2) = Q_n$$

Figure 1. Schematic of test specimen that served as basis for mathematical model.

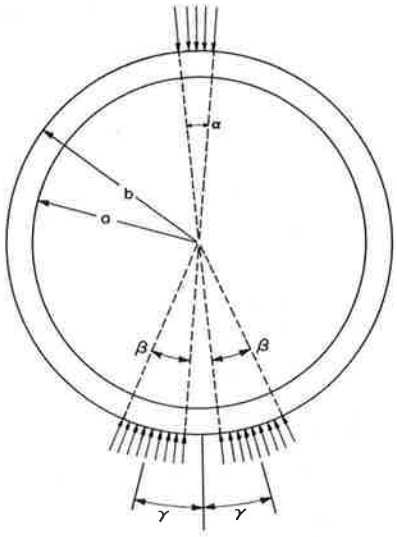

Figure 2. Three-edge bearing (wood-block) schematic.

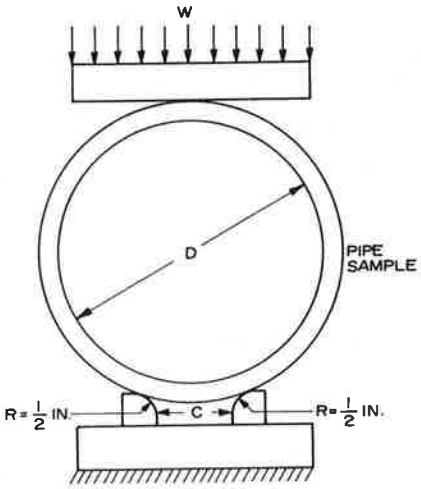

Figure 3. ISO V-block schematic.

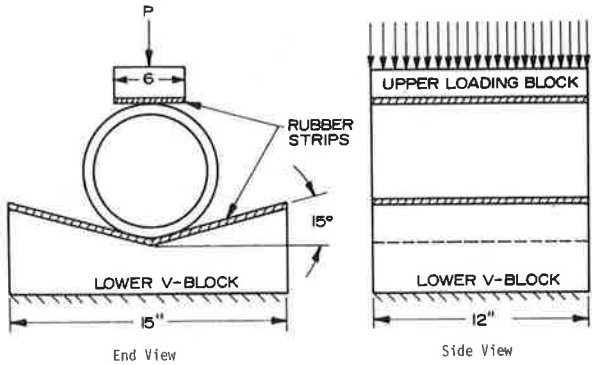

$$a_n a^{n-2}(n - n^2) + b_n a^n(n - n^2 + 2) - c_n a^{-(n-2)}(n - n^2) - d_n a^{-n}(n + n^2 - 2) = 0$$

$$a_n(n - 1)\,a^{n-2} + b_n(n + 1)\,a^n - c_n(n + 1)\,a^{-(n+2)} - d_n(n - 1)\,a^{-n} = 0$$

$$a_n(n - 1)\,b^{n-2} + b_n(n + 1)\,b^n - c_n(n + 1)\,b^{-(n+2)} - d_n(n - 1)\,b^{-n} = 0$$

The matrix form of these equations is as follows:

$$\begin{bmatrix} b^{n-2}(n - n^2) & b^n(n - n^2 + 2) & -b^{-(n+2)}(n + n^2) & -b^{-n}(n + n^2 - 2) \\ a^{n-2}(n - n^2) & a^n(n - n^2 + 2) & -a^{-(n+2)}(n + n^2) & -a^{-n}(n + n^2 - 2) \\ a^{n-2}(n - 1) & a^n(n + 1) & -a^{-(n+2)}(n + 1) & -a^{-n}(n - 1) \\ b^{n-2}(n - 1) & b^n(n + 1) & -b^{-(n+2)}(n + 1) & -b^{-n}(n - 1) \end{bmatrix} \begin{bmatrix} a_n \\ b_n \\ c_n \\ d_n \end{bmatrix} = \begin{bmatrix} Q_n \\ 0 \\ 0 \\ 0 \end{bmatrix}$$

A computer program was written that solves this system of equations for the constants a_n, b_n, c_n, and d_n and then calculates σ_θ for various loading angles and various diameter/thickness ratios.

EXPERIMENTAL PROCEDURES

Test Methods

The three-edge (wood-block) test method was conducted as described in ASTM C-500 (Figure 2). The ISO V-block test method consists of a V-shaped test block lined with rubber strips. The upper block also has a bonded rubber strip that comes in contact with the test pipe (Figure 3). In this method, the loading rate is constant and such that failure occurs in 15-30 s.

Sampling Protocol

The pipes to be tested had their pipe ends clearly marked either L (left) or R (right) to identify pipe orientation during manufacture. The pipes were then cut into 1-ft (305-mm) test sections as indicated in Figure 3. Each section was identified with a letter, starting with A on the left end of the pipe. The V's and the W's on the pipe section in Figure 4 stand for V-block and wood-block methods, respectively. That is, sections A, C, E, H, and J were tested by using the wood-block three-edge bearing method and sections B, D, G, W, and K were tested by using the V-block method.

The proposed ISO V-block test method recommends a sample length of 7.8 in (200 mm) for nominal diameters up to and including 11.8 in (300 mm) and a sample length of 11.8 in for nominal diameters above 13.8 in (350 mm). Tests were run on samples both 12 in and 8 in (203 mm) long to determine whether sample length in this range has a significant effect on the resulting crush load per unit length. Data from these tests show that resulting crush loads per unit length were essentially equal for the two sample lengths tested. Therefore, samples 1 ft in length (a common sample length in the United States) were used throughout this study.

RESULTS

Twenty-two pipe lengths of various classes and diameters were cut into samples following the procedure indicated in Figure 4. More than 100 V-block crush tests and 100 wood-block crush tests were run. Data are plotted graphically in Figures 5 and 6. Also shown in Figures 5 and 6 and in Table 1 are data from the analytical solution of the problem. Presentation of the data as in Figure 5 shows little scatter in the data. However, such a presentation hides some of the causes and effects. This can be clearly seen by plotting the same information on the (V - W)/W versus W axis (Figure 6).

Approximate mathematical models for the two test methods were determined and solutions obtained via computer programming. This was done by calculating the loading angle on the bottom of the test samples for the wood blocks. Of course, this angle varies with the outside diameter of the pipe and the wood-block spacing. Very narrow, almost line loadings were assumed. For the V-block test method the loading angle is always 15 degrees. Here the assumed loads were not applied along a line but were distributed about 10 degrees, 5 degrees each side of the contact point.

In both experimental and theoretical data, it appears that the change (V - W)/W x 100 approaches 7 percent as W gets very large. Why does a discrepancy exist between the experimental and the theoretical data? The answer is clear. The V-block method produces a higher apparent strength over the wood-block method for the following reasons:

1. The angle of loading at the bottom of the test specimen is different;
2. Due to the rubber pads, the loading has some distribution around the circumference (not a line load); and
3. Imperfections such as out-of-roundness, high spots, etc., are not so critical for the rubber-padded V-block. That is, point-load concentrations are much less likely to happen.

The mathematical model was approximate because item 3 could not be modeled even though items 1 and 2 were taken into account. Thus, the influence item 3 has on the resulting strength can be determined only experimentally. It is easily seen that statistically the experimental data points obtained from the V-block method are about 300 lbf higher than data points predicted from the theoretical solutions. This difference is due to item 3 above. The percentage influence of item 3 is relatively high for low-strength pipe, relatively low for high-strength pipe, and approaches zero for very-high-strength pipe. Thus, the experimental solution and the theoretical solution become asymptotic to the 7 percent line for very-high-strength pipes. The fact that the two solutions approach each other gives further verification that the experimental solution is correct and may be used to accurately predict V-block crush-load data from wood-block data, or vice versa. The equation correlating the two test methods is as follows (1 lbf = 0.004 kN):

$$F_V = 1.07F_W + 200\,(\text{lbf/ft}) \tag{10}$$

Figure 4. Sampling protocol: W-samples tested in three-edge bearing and V-samples tested in ISO V-block method.

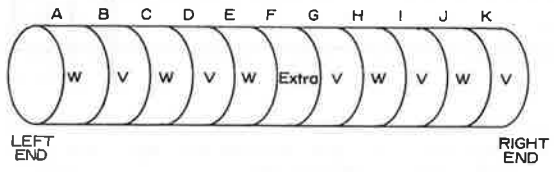

Figure 5. V-block versus wood-block strength.

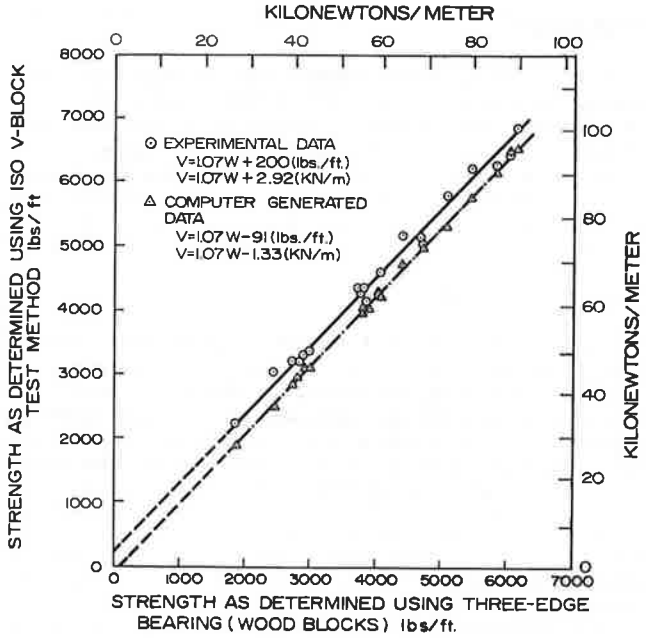

Figure 6. Apparent percentage increase in crush strength with ISO V-block test method.

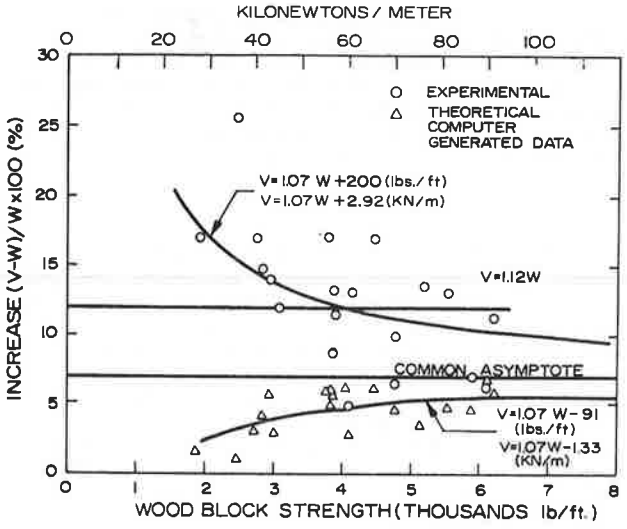

Table 1. Analytic solution for actual pipe samples tested.

Wood-Block Separation C	Diameter (in) and Class	D/t	Predicted Crush Load (lbf/ft) Wood Block	Predicted Crush Load (lbf/ft) ISO V-Block	Δ Percent
1-in spacing	4, 2400	9.9	2.454	2.479	1.0
	6, 1500	14.5	1.867	1.897	1.6
	6, 2400	12.7	4.103	4.214	2.7
	8, 1500	15.3	3.005	3.092	2.9
	8, 2400	15.8	2.736	2.815	2.9
	8, 3300	13.4	5.133	5.308	3.4
	10, 2400	16.6	2.929	3.093	5.6
	10, 3300	15.3	3.802	3.988	4.9
	12, 1500	18.7	2.822	2.941	4.2
	12, 2400	18.1	3.755	3.969	5.7
	12, 3300	14.9	3.840	4.044	5.3
	16, 3300	18.4	4.708	5.028	6.8
2-in spacing	18, 2400	17.7	4.748	4.962	4.5
	18, 3300	18.1	3.818	4.039	5.8
	18, 5000	16.3	5.501	5.754	4.6
	24, 2400	21.5	4.441	4.716	6.2
	24, 3300	20.3	4.064	4.316	6.2
	24, 5000	17.3	6.089	6.497	6.7
3-in spacing	30, TR-30	19.8	5.872	6.142	4.6
	30, 5000	19.8	6.191	6.544	5.7

Note: 1 in = 25 mm; 1 lbf = 0.004 kN.

Table 2. Load factors for asbestos cement pipe buried in either class C or class B bedding.

C-Bedding				B-Bedding	
Crush Load (lbf/ft)	Load Factor	Crush Load (lbf/ft)	Load Factor	Crush Load (lbf/ft)	Load Factor
3010	1.9	5580	1.43	2800	1.90
3500	1.32	2200	1.66	3400	1.51
5050	1.19	4900	1.24	4450	1.73
3410	1.74	2950	1.92	3800	1.77
3990	1.50	2700	1.60	5960	1.66
5580	1.28	2800	1.64	3970	1.64
4430	1.76	2800	1.74		
5910	1.24	2360	2.17		
5250	1.21	4700	1.16		
2990	1.31	6380	1.31		
2410	1.62	3900	1.54		
2500	1.60	2600	1.73		
5000	1.27	3400	1.50		
5050	1.24	3400	1.39		
5040	1.36	3350	1.50		
7000	1.07	2250	1.87		
6375	1.20	2200	2.03		
3130	1.75				
2525	1.67				

Note: 1 lbf = 0.004 kN.

Figure 7. Load factor as function of three-edge bearing crush strength.

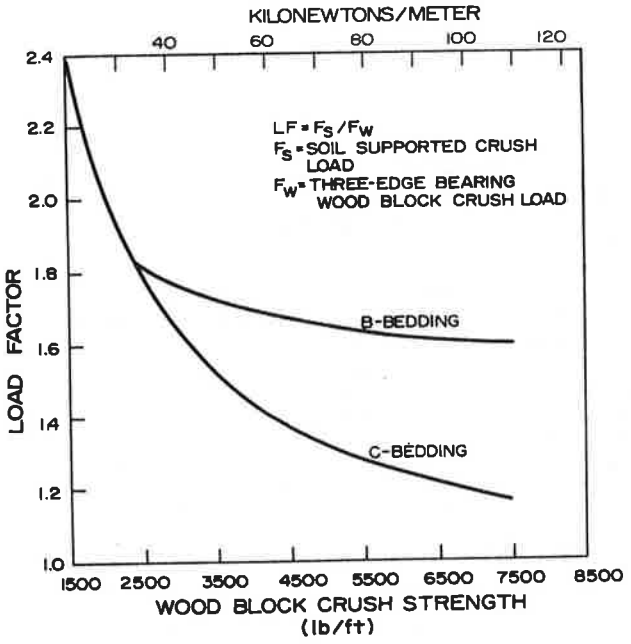

F_V represents crush load as determined by the V-block method. F_W represents the crush load as determined in the three-edge bearing (wood-block) method. This equation represents a least-squares fit to the experimental data shown graphically in Figure 5.

LOAD-FACTOR DATA FROM 1975 UTAH STATE UNIVERSITY REPORT

An experimental study was carried out at Utah State University in 1975 to determine load factors (4). In that study the load factors were determined by using the three-edge bearing (wood-block) method for determining the crush load (F_W). Similar samples were loaded in an embankment condition to determine the soil-supported crush load (F_s).

$$\text{Load factor} = LF = F_s/F_W \quad (11)$$

Data from this study are given in Table 2. Equations of the form $LF = \alpha/F_W + \beta$ were determined by using the least-squares method to determine α and β.

These equations are plotted in Figure 7. It is noted that B bedding gives little or no advantage over C bedding for low-strength pipes. It is assumed, for pipe crush strengths less than the intersection of the two curves, that the C curve applies to both C and B beddings. It is also noted that for high-strength pipes, the load factor for B bedding is about 30 percent higher than that for C bedding. The equations for the two curves that relate load factors $(LF)_W$ to wood-block bearing load (F_W) are as follows (1 lbf = 0.004 kN):

For C bedding,

$$(LF)_W = 2264/F_W + 0.87;\ F_W(\text{lbf/ft}) \quad (12)$$

For B bedding,

$$(LF)_W = 797/F_W + 1.49;\ F_W(\text{lbf/ft}) \quad (13)$$

V-BLOCK LOAD FACTORS

If the crush loads are to be determined by using the ISO V-block method, it is necessary to correct the load factors to a new base. Obviously, since V-block crush loads are larger than corresponding wood-block values, the load factors referred to the V-block base will be proportionally smaller. The load factors associated with the V-block and wood-block bases are as follows:

$$(LF)_V = F_s/F_V \quad (14)$$

$$(LF)_W = F_s/F_W \quad (15)$$

From Equation 15,

$$F_s = (LF)_W F_W \quad (16)$$

Upon the substitution of Equation 16 into Equation 14, one finds

$$(LF)_V = (LF)_W F_W/F_V \quad (17)$$

From Equation 10,

$$F_V = 1.07F_W + 200$$

Thus Equation 17 becomes

$$(LF)_V = (LF)_W F_W/(1.07F_W + 200) \quad (18)$$

From Equation 12 for C bedding, $(LF)_W = 2264/F_W + 0.87$. Thus, for C bedding, Equation 18 becomes

$$(LF)_V = (2264 + 0.87F_W)/(1.07F_W + 200) \quad (19)$$

From Equation 13 for B bedding, $(LF)_W = 797/F_W + 1.49$. Thus, for B bedding, Equation 18 becomes

$$(LF)_V = (797 + 1.49F_W)/(1.07F_W + 200) \quad (20)$$

One may use Equations 19 and 20 for calculating V-block load factors in terms of wood-block crush loads for C and B beddings, respectively.

In a similar manner, equations may be derived for calculating V-block load factors in terms of V-block crush loads. Equation 10 may be solved for F_W as follows (1 lbf = 0.004 kN):

$$F_W = (F_V - 200)/1.07\ (\text{lbf/ft}) \quad (21)$$

F_W from Equation 21 and $(LF)_W$ from Equation 12 may be substituted into Equation 17 to arrive at the following for C bedding (1 lbf = 0.004 kN):

$$(LF)_V = (2101/F_V) + 0.81; F_V(lbf/ft) \quad (22)$$

Similarly, F_W from Equation 21 and $(LF)_W$ from Equation 13 can be substituted into Equation 17. The result is the following equation for B bedding (1 lbf = 0.004 kN):

$$(LF)_V = (518/F_V) + 1.39; F_V(lbf/ft) \quad (23)$$

REFERENCES

1. M.G. Spangler and R.L. Handy. Soil Engineering, 3rd ed. Intext Educational Publishers, New York, 1973.
2. Design and Construction of Sanitary and Storm Sewers. In ASCE Manual and Report on Engineering Practice No. 37 (WPCF Manual of Practice No. 9), American Society of Civil Engineers and Water Pollution Control Federation, New York, 1973, pp. 210-211.
3. S.P. Timoshenko and J.N. Goodier. Theory of Elasticity, 3rd ed. McGraw-Hill, New York, 1970.
4. R.K. Watkins. A.P. Moser, and O.K. Shupe. Soil Supported Strength of Buried Asbestos Cement Pipe. Buried Structure Laboratory, Utah State Univ., Logan, 1976.

Publication of this paper sponsored by Committee on Culverts and Hydraulic Structures.

Rigid Pipe Prooftesting Under Excess Overfills with Varying Backfill Parameters

RAYMOND E. DAVIS AND FRANK M. SEMANS

Field testing and analyses of two culverts at Cross Canyon are described: a 96-in prestressed-concrete functioning culvert under 200 ft of overfill and an 84-in reinforced-concrete dummy culvert under a maximum 183-ft overfill in the same embankment. Eight instrumented and two noninstrumented zones in the dummy pipe and functional and unstressed control instrumented zones of the prestressed pipe were monitored during and after embankment construction to determine peripheral soil stresses, internal forces, and displacements. Correlations were established between quasi-theoretical and measured parameters (moments, thrusts, displacements, distress, etc.) with a programmed analysis. Some standard analytical tools (settlement ratio, finite element) were checked against observations, and relative costs of different construction modes were considered. Heger's recently developed criteria were checked against actual appearances of two of four distress modes. The programmed analysis was modified to predict these distress modes. Profiles of effective-density coefficients were established for various construction modes. The importance of designing for density distributions representative of contemplated construction modes is emphasized.

A comprehensive 15-year research program pertinent to structural behavior of culverts embedded in deep embankments (100+ ft) conducted by the California Department of Transportation (Caltrans) Structures Design Research Unit has been described (1-25). Eight papers (8,12,13,15-17,19,20) have discussed field tests of two reinforced-concrete pipe culverts at Mountainhouse Creek: a grossly underdesigned 1000D 84-in-diameter dummy culvert and (17) a functional 4000D 96-in-diameter pipe. Each pipe included six zones to be subjected to varying bedding and backfilling parameters. Buried under a 137-ft overfill (almost nine times the 16-ft maximum stipulated by current specifications), several zones of the dummy culvert responded encouragingly to specialized embedment techniques.

Tests of additional bedding and backfill parameters and pipe segments of varying strengths were conducted at Cross Canyon, near Sunland, California, to establish more realistic functional relationships between pipe strengths and allowable limiting overfills. Again, a functional culvert and a dummy pipe were tested.

Designed for 200 ft of overfill, the functional culvert is of 96-in diameter and 23.5-in wall thickness with two layers of closely spaced prestressing wires. Tests of one pipe segment (Zone 11) are described later.

The 84-in-diameter dummy culvert, its invert located 13 ft above the crown of the functional culvert at varying horizontal distances therefrom, was divided into 10 zones (Figure 1); pipe strengths and bedding and backfill parameters are as shown in Figures 2 and 3. Dummy pipe segments except those in Zones 5 (1750D), 6 (2500D), and 7 (3600D) were nominally classified as having a 1000D load rating; measured load ratings, based on tests of three pipe segments of each pipe strength, were Zones 1-4 and 8-10, 997D; Zone 5, 1910D; Zone 6, 2574D; and Zone 7, 3780D.

In all instrumented zones except Zone 1, at least one 8-ft-long pipe segment was placed on either side of the instrumented segment as a buffer segment where Method-A (ordinary embankment material) backfill was employed. Two segments were used in the zones (8, 9, and 10) with Method-B (low-modulus inclusion) backfill.

DESCRIPTION OF INSTRUMENTATION

Dummy culvert instrumentation design was influenced by observed behavior of culverts and instrumentation in earlier projects, briefly described as follows (Figures 4 and 5):

1. Symmetry of soil stress distribution has never been observed in Caltrans culvert research.
2. Integrated forces acting on pipe peripheries, based on measured soil stresses, have indicated vertical force unbalance often measured in tens of kips.
3. Failures of interface stress meters in sensitive locations or inconsistencies in measured stresses due to soil heterogeneity have often greatly decreased confidence in overall results.